Illumination Invariance and Object Model in Content-Based Image and Video Retrieval

Ze-Nian Li   Osmar R. Zaïane   Zinovi Tauber
School of Computing Science
Simon Fraser University
Burnaby, B.C., Canada V5A 1S6
{li, zaiane, zinovi}@cs.sfu.ca

Abstract

With huge amounts of multimedia information connected to the global information network (Internet), efficient and effective image retrieval from large image and video repositories has become an imminent research issue. This article presents our research in the C-BIRD (Content-Based Image Retrieval in Digital-libraries) project. In addition to the use of common features such as color, texture, shape and their conjuncts, and the combined content-based and description-based techniques, it is shown that (a) color–channel–normalization enables Search by Illumination Invariance, and (b) feature localization and a three-step matching algorithm (color hypothesis, texture support, shape verification) facilitate Search by Object Model in image and video databases.

Keywords: Color, Content-based retrieval, Digital library, Feature localization, Generalized Hough Transform, Image and video databases, Modeling and matching, Segmentation, Shape, Texture.

1 Introduction

Image and video indexing and retrieval has lately drawn the attention of many researchers in the computer science community [1, 2, 3, 4, 5, 6, 7, 8, 9]. With the advent of the World-Wide Web (WWW), research in computer vision, artificial intelligence, databases, etc. is taken to a larger scale to address the problem of information retrieval from large repositories of images. Previous pattern recognition and image analysis algorithms in the vision and AI fields dealt with small sets of still images and did not scale. With large collections of images and video frames, scalability, speed and efficiency are the essence for the success of an image and video retrieval system.

There are two main families of image and video indexing and retrieval systems: those based on the content of the images (content-based) like color, texture, shape, objects, etc., and those based on the description of the images (description-based) like keywords, size, caption, etc. While description-based image retrieval systems are relatively easier to implement and to design user interface for, they suffer from the same problems as the information retrieval systems in text databases or Web search engines. It has been demonstrated that search engines using current methods based on simple keyword matching perform poorly. The precision[1] of these search engines is very low and their recall[2] is inadequate. It has been demonstrated in [10] that any single web search engine provides the user with only 15-42 % of the relevant documents. Furnas, et al. [11] show that due to widespread synonymy and polysemy in natural languages, indexing methods based on the occurrence of single words do not perform adequately.

Content-based image retrieval systems use visual features to index images. These systems differ mainly in the way they extract the visual features and index images, and the way they are queried. Some systems are queried by providing an image sample. These systems search for similar images in the database by comparing the feature vector (or signature) extracted from the sample with the available feature vectors. The image retrieval system Image Surfer provided by Yahoo, for example, is based on this type of search. Other systems are queried by specifying or sketching image features like color, shape or texture, which are translated into a feature vector to be matched with the known feature vectors in the database. QBIC [2] and WebSeek [7], for example, provide both sample-based queries and the image feature specification queries. WebSeer [12] on the other hand, combines image descriptions, like keywords, and image content, like specifying the number of faces in an image, and uses image content to distinguish between photographs and figures. However, the visual features extracted are very limited. Another major difference between image retrieval systems is in the domain they index. While Virage [4] indexes solely image databases, using COIR (Content-Oriented Image Retrieval) [13], AMORE (Advanced Multimedia Oriented Retrieval Engine) [9] indexes images from the World-Wide Web. Content-based systems give a relatively satisfactory result with regard to the visual clues, however, their precision and recall are still not optimized.

[1] Precision—the ratio of relevant documents to the total number of documents retrieved.

[2] Recall—the percentage of relevant documents among all possible relevant documents.

Effective strategies for image retrieval will benefit from exploiting both content-based and description-based retrieval techniques, and will combine conjunctions and disjunctions of image features and descriptions in the queries, as well as providing users with adequate and efficient user interfaces for both querying and browsing.

We have been developing the C-BIRD (Content-Based Image Retrieval in Digital-libraries) system, which combines automatically generated keywords and visual descriptors like color, texture, shape, and feature localization, to index images and videos in the World-Wide Web. This paper presents our new results of *Search by Illumination invariance*, *Search by Object Model* and the discussion of *feature localization* vs. image segmentation.

Swain and Ballard's work on color object recognition by means of a fast matching of color histograms [14] began an interest in the use of simple color–based features for image and video database retrieval. In this method, a database of coarse histograms indexed by three color values is built up. A very simple and fast histogram matching strategy can often identify the correct match for a new image, or a near–match, by using an L1 metric of histogram differences[14]. It was soon realized that, along with confounding factors such as object pose, noise, occlusion, shadows, clutter, specularities, and pixel saturation, a major problem arose because of the effect of changing illumination on images of color objects [15]. After all, it would be quite natural for an object in a database to be presented as it appears imaged under some other lighting.

Several color object recognition schemes exist that purport to take illumination change into account in an invariant fashion. In [16], we address the problem of illumination change by extending the original Swain and Ballard method to include illumination invariance in a natural and simpler way than heretofore. First, it is argued that a normalization on each color channel of the images is really all that is required to deal properly with illumination invariance. Second, with an aim of reducing the dimensionality of the feature space involved, a full–color (3D) representation is replaced by 2D chromaticity histograms. It is shown that the essential illumination–invariant color information is maintained across this data reduction. The normalization step has the effect of undoing a changing–illumination induced shift in pixel color–space position and in chromaticity space.

Histograms in chromaticity space are indexed by two values, and are treated as though they were images. In order to greatly improve the efficiency in searching large image and video databases, the chromaticity histogram-images are compressed and then indexed into a database with a small feature vector based on the compressed histogram. In the current implementation the chromaticity histogram-image is first reduced by using a wavelet scaling function. Then, the Discrete Cosine Transform (DCT) is applied, followed with a zonal coding [17] of the DCT image. This results in an effective low–pass filtering of the chromaticity histogram. The resulting indexing scheme is very efficient in that it uses a DCT-chromaticity vector of only 36 values. We have also applied this technique to video segmentation [18]. Since it is much more frequent that illumination changes due to camera motions and object motions in video, our color-channel-normalization method is shown to clearly outperform other cut-detection methods that only rely on color histograms.

Most existing techniques for content-based image retrieval rely on global image features such as color and texture. These global methods are based on simple statistics extracted from the entire images. They are easy to obtain and to store in a database, and their matching takes little time. Inevitably, the global methods lack the power of locating specific objects and identifying their details (size, position, orientation, etc.). Some extensions to the global method include search by color layout [2], by sketch [6, 9], and by color regions according to their spatial arrangements [7, 8].

It has long been argued that *segmentation* plays an important role in human vision [19]. Ever since the 60s and 70s, *image segmentation* has been one of the most persistent research areas in computer vision. It is hoped that recognition would become much easier after segmentation. However, it is well-known that a good image segmentation is often impossible to attain. Commonly, images are either "over-segmented" or "under-segmented". As Marr [20] pointed out, "... the difficulties in trying to formulate what should be recovered as a region from an image are so great as to amount almost to philosophical problems." In [21] it is argued that like many vision problems, the problem of image segmentation is "ill-defined".

Realizing the inadequacy of global features and methods such as the color histogram (or texture) for content-based image retrieval, more and more researchers have proposed image segmentation (based on color, texture, and shape) [7, 8, 22] as a main step toward an effective content-based image retrieval. Apparently, as long as a good segmentation is obtained, powerful constraints such as *spatial relationships* can be enforced. To overcome the difficulties in achieving a sound segmentation, heuristics such as size-of-the-region and maximum-number-of-the-regions are naturally developed to avoid over-segmentation; also, motion in the spatiotemporal domain is exploited to improve image segmentation in video

[8].

This paper argues that, in spite of its popularity, the traditional image segmentation is not a good image preprocessing tool for the content-based retrieval from image and video databases. Instead, a new approach of *feature localization* is proposed. Based on the *locales* extracted from the feature localization, a three-step algorithm that employs color hypothesis, texture support, and shape verification is developed. Since the first two steps enable the estimation of the size, orientation, and location of the object, the use of the Generalized Hough Transform (GHT) in the last step becomes very efficient and viable.

In contrast to most existing approaches, our work has the following characteristics: (a) the use of color–channel–normalization for illuminant-invariant image and video retrieval, (b) the exploitation of intrinsic and compact feature vectors and the three-step matching algorithm for search by object model, and (c) the exploration of feature localization in content-based image and video retrieval.

The remainder of this paper is organized as follows. In Section 2, we describe the illumination-invariant color indexing technology based on chromaticity of the normalized images. The discussion of feature localization vs. image segmentation is in Section 3. Section 4 presents the modeling and matching techniques. Section 5 describes the experimental results. Section 6 summarizes our conclusions and future enhancements.

2 Illumination-Invariant Color Indexing

In this section it is shown that a simple color indexing method that is efficient and invariant under illuminant change can be derived for Search by Illumination Invariance if we store a representation of a chromaticity histogram for each image that is first normalized, reduced in size by a wavelet transformation, and then further reduced by going to the frequency domain and discarding higher–frequency DCT coefficients.

2.1 Chromaticity histogram of color–channel–normalized image

Define the chromaticity (r, g) for each pixel by [23]

$$r = R/(R+G+B) \quad , \quad g = G/(R+G+B) \tag{1}$$

The chromaticity is the projection of an RGB triple onto the planar triangle joining unit distance along each of the color axes. It is important to note that, although the definition of the chromaticity immediately provides some normalization, i.e., $r + g + b = 1$ if b is defined accordingly, and it provides invariance to the intensity of the light by dividing by the sum of the three color bands, the usage of chromaticity itself is insufficient for illumination invariance when the color (chrominance) of the light changes.

A color–channel-normalization method was proposed in [16]. Given an image of size $m \times n$, each of the RGB channels is treated as a long vector of length $m \cdot n$. It is shown in [16] that by employing an L2 normalization on each of the three RGB vectors, the effect of any illumination change is approximately compensated. The color–channel–normalization step effectively accomplishes illumination invariance. The usage of chromaticity provides two additional advantages: (a) the color space is reduced from 3D (e.g., RGB, HSV, etc.) to 2D, hence less computations, (b) the chromaticity value is indeed guaranteed to be in the range of [0, 1.0]; this helps the formation of a small (well-bounded) 2D histogram space later.

From the chromaticity image, a chromaticity histogram can be obtained. This histogram itself is viewed as a *histogram-image*, i.e., each bin value is viewed as a pixel value. Some image compression techniques will then be applied to this histogram image. Note that since $r + g \leq 1$, the chromaticity entries must lie below the main diagonal, thus only half of the pixels in the histogram-image are used.

2.2 Histogram intersection

In [14], a very useful histogram metric is developed, which we adopt in C-BIRD for both the usual color histogram matching and the uncompressed chromaticity histogram matching.

Adapting Swain and Ballard's definition to the present situation, we define the intersection of chromaticity histograms $\boldsymbol{H}_a$ and $\boldsymbol{H}_b$ as:

$$\mu \;\equiv\; \sum_{i,j} min\{\boldsymbol{H}_a(i,j), \boldsymbol{H}_b(i,j)\} \tag{2}$$

Swain and Ballard normalize intersection (or match) values by the number of pixels in the model histogram, and thus matches are between 0 and 1. Alternatively, one can make the volume under each histogram equal to unity, effectively making each image have the same number of pixels and turning the histogram into a probability density. Time for histogram intersection is proportional to the number of histogram bins, and so is very fast.

It can be shown that histogram intersection is equivalent to 1 minus an L1 distance, and so $(1 - \mu)$ forms a metric δ, with $\delta = 1 - \mu = (1/n) \sum |\boldsymbol{H}_a - \boldsymbol{H}_b|$, where n is the number of histogram bins. The utility of this metric is that it helps to alleviate the effects of noise in the following way. suppose an image has significant noise and it does not occur in the particular model image chromaticity histogram being compared to, then such noise values might tend to dominate, in an L2, squared–differences norm. Instead, here, zero occurrences in the model histogram are counted and such effects do not contribute to the metric.

Content-based retrieval proceeds by intersecting the chromaticity histogram of an unknown object with similar histograms precomputed and stored in a database. The highest value of μ, or in other words the smallest distance value $(1 - \mu)$ indicates the database image that matches best.

2.3 Chromaticity histogram–image compression

Chromaticity histogram matching without compression could be computationally intensive. We would like to recover an accurate approximation of histogram–images without sacrificing efficiency. As a guiding principle it would also be sensible to maintain a linear relationship between the histogram–image and its compressed representation. We can adhere to this principle by applying only linear operations while compressing the histogram–images. Therefore, here we first apply a linear low–pass filter to both histogram–images, resulting in new histograms $\boldsymbol{H}$ and $\boldsymbol{H}'$. To best approximate the chromaticity histograms, the low–pass filtered histogram–images should approximate the original ones as closely as possible, yet be of lower resolution. The scaling function of bi-orthonormal wavelets, as a symmetrical low–pass filter, can be exploited to that end. Basically, scaling functions with more "taps" use polynomials of higher order to approximate the original function (the number of taps is the number of nonzero coefficients) [24]. Our main concern is to capture the most detail but in lower resolution. In [16], a good balance is achieved between efficiency and precision by using the symmetrical 9–tap filter.

After applying the scaling function several times to the original histogram–images, assuming for simplicity square histogram–images with resolution $2^n \times 2^n$, the size 16×16 lower resolution histogram–images are obtained.

Now consider the DCT: if we denote the result of $\boldsymbol{H}$ transformed via a DCT by $\widehat{\boldsymbol{H}}$, then since the DCT is linear we could confidently index on $\widehat{\boldsymbol{H}}$.

Since the lower frequencies in the DCT capture most of the energy of an image, after applying the DCT we can retain just the lower frequency coefficients for histogram–image database indexing with fairly good accuracy — a very effective and efficient way of realizing a further low–pass filtering. By experiment [16] it is found that using only 36 coefficients worked well, these being those in the first 36 numbers in the upper left corner of the DCT coefficient matrix[3].

Denote by $\boldsymbol{H}_d$ 36 values derived from the first 36 DCT coefficients. We index on the L2 distance between $\boldsymbol{H}_d$ for the model histogram–image and that for the test histogram–image.

Populating the database, then, consists of calculating off-line the 36 values $\boldsymbol{H}_d$, viewed as indices for each model image. For image query, first the 36 values for the query image are computed, thus obtaining $\boldsymbol{H}'_d$; then for every model image, the L2 distance $[\sum(\boldsymbol{H}'_d - \boldsymbol{H}_d)^2]^{1/2}$ is calculated. The model image minimizing the distance is taken to be a match for the query image.

Note that in this method only reduced, DCT transformed, quantized histogram–images are used — no inverse transforms are necessary and the indexing process is carried out entirely in the compressed domain.

The choice that the reduced resolution of the wavelet chromaticity histogram–images be 16×16 and that the number of DCT coefficients retained be 36 is made quite empirically. Detailed analysis and some variation of the choice of the DCT coefficients are provided in [16].

3 Feature Localization vs. Image Segmentation

3.1 Definition of region revisited

Image segmentation is a process to segment an entire image into disjoint regions. A region consists of a set of pixels that share certain properties, e.g., similar color (or gray-level intensity), similar texture, etc. As in [25], if R is a region,

1. R is *connected*, iff all pixels in R are connected [4],

2. $R_i \cap R_j = \phi, \quad i \neq j$,

[3] Instead of using a conventional 8×8 window for the DCT, a 16×16 window is adopted. As a result, a finer resolution (twice as high as with 8×8) in the spatial frequency domain is realized. Since the low–pass filtering after DCT can only retain a limited number of coefficients for efficiency, the net effect of having a larger (16×16) window is that a more detailed parameterized description at the lower end of the spectrum is facilitated. This is beneficial when very low–resolution wavelet images are used for matching in our method.

[4] Either 4-connected or 8-connected. See [25] for more details.

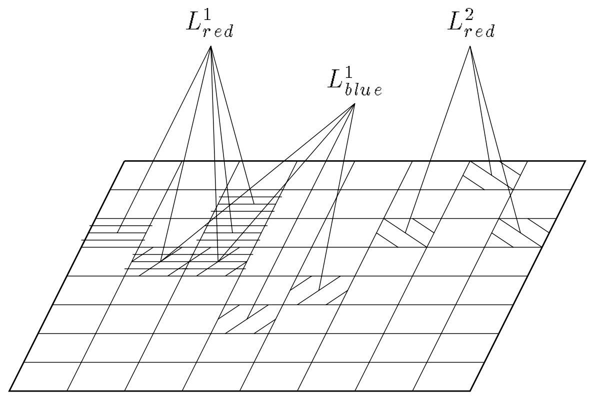

Figure 1: An image of 8×8 tiles, and locales for colors red and blue.

3. $\cup_{k=1}^{m} R_k = I$, the entire image.

Although regions do not have to be connected, most available region-based and/or edge-based segmentation methods would yield connected regions, and it is error-prone to merge some of them into non-connected regions. In short, the traditional segmentation algorithms assume (1) regions are mostly *connected*, (2) regions are *disjoint*, (3) segmentation is *complete* in that any pixel will be assigned to some region, and the union of all regions is the entire image.

Such a segmentation algorithm will yield more than a dozen purple regions, one for each character, for the title of the book shown in Fig. 7(A). It will also yield (unexpectedly) many white regions, since all the white blobs inside the letters 'A', 'P', 'R' 'O' will unfortunately be identified as regions unless some really effective algorithm can identify them as belonging to a non-connected region together with the two white boxes. The above example, albeit simple and not at all unusual, indicates that the traditional image segmentation does not yield useful grouping and representation for object recognition.

3.2 Locale for feature localization

We argue that a more useful and attainable process is feature localization that will identify features by their locality and proximity. A new concept *locale* is hence defined. Locales use squares of pixels (*tiles*) instead of pixels as their smalles unit at the image level.

Definition: A *locale* $\mathcal{L}_x$ is a local enclosure (or locality) of feature x.

$\mathcal{L}_x$ has the following descriptors:

- envelope L_x — a set of tiles to represent the locality of $\mathcal{L}_x$.

- geometric parameters — *mass* $M(\mathcal{L}_x)$, *centroid* $\mathbf{C}(\mathcal{L}_x)$, *eccentricity* $E(\mathcal{L}_x)$, and shape parameters for the locale, etc.

A tile is a square area in an image, its size is chosen as 16×16 pixels in this paper. Tile is the building-unit for envelopes. A tile is 'red' if a sufficient number of pixels (e.g., 10%) within the tile are red. It follows that a tile can be both 'red' and 'blue' if some of its pixels are red and some are blue. While pixel is the building-block for image segmentation, tile is the building-block for feature localization. Tiles are grouped into an envelope, if they are geometrically close. The closeness will be measured by eccentricity and distance to be discussed below.

Fig. 1 shows a square image that has 8×8 tiles, two locales for color red, and one locale for color blue. The envelope L^1_{red} in Fig. 1, for example, consists of 5 tiles.

$M(\mathcal{L}_x)$ is the number of pixels in L_x that actually have feature x, e.g., the number of pixels that are red. $M(\mathcal{L}_x)$ is usually less than the Area of L_x, although it could be equal to it. $\mathbf{C}(\mathcal{L}_x)$ is simply the centroid of the mass. $E(\mathcal{L}_x)$ is a measure of the average distance from pixels in L_x to the centroid, it measures the eccentricity of $\mathcal{L}_x$. Note, M, $\mathbf{C}$, E, etc. are measured in unit of pixels, not in tiles. This guarantees the granularity. Hence the feature localization is not merely a low-resolution variation of image segmentation.

The procedure for generating the locales basically uses *merge*. First, simple statistics (M, $\mathbf{C}$, E) is gathered within each tile. Afterwards, a method similar to "pyramid-linking" [26] is used to merge the tiles into locales. In terms of the parent-child relation, the overlapped pyramid is used.

Working bottom-up, all tiles having feature x are linked to their parent and merged into $\mathcal{L}_x$ if the merged locale will have $E(\mathcal{L}_x) < \tau$, where τ is a threshold normalized against $M(\mathcal{L}_x)$. Otherwise, they will be linked to two different parents belonging to different envelopes L^i_x and L^j_x. During the merge, $M(\mathcal{L}_x)$, $\mathbf{C}(\mathcal{L}_x)$, and $E(\mathcal{L}_x)$ are updated accordingly.

From the above definition, it is important to note that in the most cases the following are true:

1. $(\exists x)\mathcal{L}_x$ is *not connected*,

2. $(\exists x)(\exists y)\mathcal{L}_x \cap \mathcal{L}_y \neq \phi, \quad x \neq y$,

3. $\cup_x \mathcal{L}_x \neq I$, the entire image.

Namely, (1) pixels inside a locale for some feature are not necessarily connected, (2) locales are not always disjoint, their envelopes can be overlapped, (3) not all pixels in an image must be assigned to some locale in the feature localization process.

Locale is not simply a variant of non-connected region, the main difference between locale and non-connected region is illustrated by the above property (2). In the proposed feature localization, it is the approximate location that is identified, not the precise membership as which pixel belongs to which region. The difference is not a philosophical one. If indeed only some simple process is to be applied, e.g., template matching, then the precise membership of the region is important. In the domain of content-based image retrieval where a very large amount of image and video data are processed, such simple and precise matches are not feasible. Instead, a more heuristic (evidential) process is going to be adopted which usually involves multiple features and their spatial relationships. For this purpose, it should be evident that the 'blobby' locales are easier to extract, and more appropriate than regions formed by (connected) pixels.

Property (3) indicates that, unlike the image segmentation, the feature localization is incomplete. Use color localization as an example, we will likely not be interested in all colors or all color spots in an image, at least not some tiny noise spots. When only the locales of the few prominent colors are identified, the union of them is not the whole image.

3.3 Specifics for extracting locales

The tasks involved in extracting Locales are (1) Image tile generation and (2) envelope growing. The following is a detailed description of the tasks for identifying color locales:

3.3.1 Image tile generation

Tile size was chosen to be 16×16, because it is large enough to generate meaningful statistics for the underlying features, but also small enough to guarantee the granularity[5]. The choice of the tile size will of course be dependent on the image resolution. If a lower-resolution image is chosen, the tile size can readily be reduced to e.g., 8×8.

Color pixels in a tile are classified as of *dominant color* or *transitional color*. The transitional color often occurs between two color regions, simply because of the smooth color

[5]The size 16×16 happens to be the size of the macroblocks for the MPEG motion vectors. Although not addressed in this paper, this has been proven convenient in our current work when motion parameters are brought in consideration for retrieving the MPEG videos.

transition in the sensory data. It could also be due to the anti-aliasing effect or noise.

The dominant color is identified by comparing the intensity value of the current pixel to its 8 immediate neighbors. The criterion is that it is not on a slope of rising/declining intensity values (with a chosen threshold 10).

While identifying dominant pixels, their geometry data are also gathered in the same pass. At this initial stage, each tile is considered as a Locale.

- $M(\mathcal{L}_f)$ = count of the pixels having feature f.
- $\mathbf{C}(\mathcal{L}_f) = \frac{\sum_{i=1}^{M(\mathcal{L}_f)} \mathbf{P}}{M(\mathcal{L}_f)}$, where $\mathbf{P}$ is the point coordinate.
- $E(\mathcal{L}_f) = \frac{\sum_{i=1}^{M(\mathcal{L}_f)}((P_x - C_x(\mathcal{L}_f))^2 + (P_y - C_y(\mathcal{L}_f))^2)}{M(\mathcal{L}_f)} = \frac{\sum_{i=1}^{M(\mathcal{L}_f)}(P_x^2 + P_y^2)}{M(\mathcal{L}_f)} - C_x(\mathcal{L}_f)^2 - C_y(\mathcal{L}_f)^2$, where C_x, C_y, P_x, P_y are the x and y coordinates for $\mathbf{C}$ and $\mathbf{P}$ respectively.

  As shown above, the intermediate data generated is just $\sum_{i=1}^{M(\mathcal{L}_f)}(P_x^2 + P_y^2)$ which can be calculated efficiently in a progressive manner.

Dominant colors and associated geometric statistics are added to a tile color list. Dominant pixel geometry data is added to the first element with similar color to it in the color list, and a weighted color average is performed on the list element to obtain a better color definition. If no element with similar color exists, then a new element is created in the list for that pixel containing only its color and geometry information. Similar colors are contained in the same volume set of a $32 \times 32 \times 32$ box in a $256 \times 256 \times 256$ RGB space.

After all the dominant colors have been added to the color list, the list is sorted by $M(\mathcal{L}_f)$ in descending order, so that transitional colors have a chance to match first to the most frequent dominant color.

Next, the pixels with transitional colors are being added to the tile color list. We compare every transitional pixel i against its neighborhood of 5×5 pixels. If any of the neighbors have dominant colors then the neighbor pixel chosen is that which has a color of minimum Euclidean distance in RGB space from pixel i. The geometry statistics of pixel i are added to the color list element with the closest color to the chosen pixel, but the color information of pixel i is ignored, rather than being averaged with the list element color. If none of the neighbors of pixel i has dominant colors then the pixel i will be added to a transitional color list.

Finally, both color lists are checked for elements with similar color to other elements in the same list, which is possible because after performing the color averaging, the color can gradually change to be similar to other colors in the list. All similar elements are merged together. However, there cannot be any similar elements between the two lists, so to merge the two color lists we only need to append the transition colors list to the end of the dominant colors list.

3.3.2 Envelope growing

Generating Locales (or final envelopes) requires the use of a dynamic pyramid linking procedure. A 4×4 overlapped pyramid structure [26] is used, and parent nodes compete for links to child nodes in a fair competition.

The tile list for the image is considered as an enumeration of the pyramid child nodes, each containing a color list with associated geometry and envelope information. To obtain a fully linked pyramid, and therefore a final color list for the single top-most parent node – which is a Locales list, we apply a linking procedure iteratively until we reach the level with only one node.

PROCEDURE Envelope Growing by Pyramidal Linking:

```
begin
    Initial Linking Step:
    /* (Use 2 × 2 non-overlapped pyramid in which each child has only one parent */
        For each child node
            For each e ∈ {color list elements of the child node}
                For each similar color element pe of the parent node
                    C = the eccentricity of merged e and pe
                    If C < τ (a pyramid level dependent threshold)
                        Merge the color and geometry statistics of e into pe;
                        Make a parent-child link between e and pe;
                        /* One link only for each e at this initial stage. */
                        Break (from the last For loop);
                If e is not linked
                    Create a new node pe in the parent's color list;
                    Make a link between the child and the parent.
    Link Updating Step:
    /* Use 4 × 4 overlapped pyramid in which each child has four parents */
        Repeat until child-parent links do not change anymore
            For each child node
                For each e ∈ {color list elements of the child node}
```

Find all similar color elements pe's from 4 parent nodes;
If merging with one of the pe's yields a more compact locale than the currently linked pe
Switch e's parent to the new pe and update the statistics.

Finalization Step:

Merge similar colors and remove empty entries from parent list.
Go up one more level in the pyramid and repeat the above.

end

During each iteration in the link updating step, the parent list nodes must remain constant, so that the linking procedure is consistent in each iteration. Updating of the geometry statistics is done on an additional tentative parent list, and after the iteration the parent list is updated.

Obviously, merging criteria are needed so that the linking procedure will produce good spatial envelopes and terminate. We observe that if there is a closer choice in terms of actual pixel distance between two color list elements' centroids, it is visually and conceptually more likely to be a part of the same feature of the image. Thus, the criterion is compactness, and the competition is for the closest parent with similar features to a child. That would also guarantee termination of the linking procedure, since the overall distance of all the nodes keeps getting smaller in at least pixel size steps. It is possible that a closer parent would actually create a more disperse envelope than features are likely to exhibit, so we require that the normalized eccentricity be less than a threshold. The eccentricity is normalized by the shape and mass (M) of the color element. We analyze two extreme cases of acceptable shapes and mass in order to obtain an estimate of the magnitude of the normalized eccentricity.

If the shape is a circular disk of radius r_0 then

$$E = \sum_{r=0}^{r_0} \frac{2\pi r \times r^2}{\pi r_0^2} = \frac{1}{2}\left(r_0 + 1\right)^2 = \frac{M}{2\pi} + \sqrt{\frac{M}{\pi}} + \frac{1}{2}. \tag{3}$$

The normalized eccentricity is therefore approximately $\frac{1}{M}E$.

If the shape is a bar-like region of width $2x_0 + 1$ and height 1,

$$E = \sum_{x=0}^{x_0} \frac{2 \times x^2}{2x_0 + 1} = \frac{1}{3}\left(x_0 + 1\right)x_0 = \frac{M^2 - 1}{12}. \tag{4}$$

The normalized eccentricity is therefore approximately $\frac{1}{M^2}E$.

As derived, the circular disk's normalized eccentricity is

$$\hat{E}(M) = \frac{1}{M}E = \frac{1}{2\pi} + \sqrt{\frac{1}{\pi M}} + \frac{1}{2M}. \qquad (5)$$

We argue that the larger the locale is, the less sensitive it is to noise or holes, and therefore it should approach the most compact eccentricity possible, which is that of the circular disk. So the above equation specifies a threshold that is valid for all locale shapes with significant mass. Also, since small locales are more sensitive to noise and shape, the above equation will not apply, so we would like to assign them a higher threshold to allow more leniency in the merging. Using $\hat{E}(M)$ as a basis function, we multiply it by another function $G(M)$ of the form: $G(M) = 1 + C_1 e^{-\mu_1 M}$. This exponential function has the property that it approaches 1 when M is very large, so the product would equal $1/2\pi$. However, when M is small, the function exponentially increases the threshold required for a very compact region based on the locale size. After multiplying, the function that we get is asymptotically, and characteristically for small M, equivalent to $\frac{1}{2\pi} + C_2 e^{-\mu_2 M} = \frac{1}{2\pi} + 1.76e^{-0.00025M}$. The parameters (C, μ) were estimated based on empirical data.

The merging procedure is simply an adjustment of the envelope and a geometric correction, which can be done because the intermediate statistics are retrievable from the final statistics.

Locale extraction for all images in the database is not made at run time but before any search query is submitted. Locales are essentially used for the search by object model described in the next section. Locales for a given object model are extracted at run time when the object is presented by the user.

4 Search by Object Model

This section describes our method for Search by Object Model. A *recognition kernel* [27] is defined as a multi-resolution model for each object. Features of an object are extracted at levels that are most appropriate to yield only the necessary yet sufficient details. Together they form the kernel. Beside its multi-resolution nature, which will not be emphasized in this paper, the recognition kernel encompass intrinsic features such as color, texture, and shape which are vital for the retrieval of objects. The following two subsections describe our approaches to *modeling* and *matching* respectively, and Section 4.3 provides further implementation details.

4.1 Color, texture, shape in object modeling

1. Color: Colors in a model image are sorted according to their frequency (number of pixels) in the RGB color histogram. The first few (e.g., five) are called *Most Frequent Colors* (MFCs). When color is extracted from relatively low resolution images where only very few prominent colors are preserved, the MFCs become especially dominant.

   Locale(s) for each MFC in the object model will be extracted first. Each pair of the centroids for two of the MFC locales can be connected to produce an *MFC vector*. The length of the MFC vectors and the angles between them characterize the color distribution, size, and orientation of the object. To reduce the total number of MFC vectors, only the vectors that connect the first MFC centroid to the other MFC centroids are used. Hence, for k ($k \geq 2$) MFCs, the total number of MFC vectors is $k - 1$.

   For simplicity, the RGB color model is adopted. It suffices for the purpose of the content-based retrieval in C-BIRD. Alternatively, some luminance-chrominance color models (e.g., YUV, LUV) can be used which would reduce the representational redundancy present in the RGB model.

2. Texture: As the color histogram can be defined in a 3D space (RGB, LUV, etc.), texture histogram can also be defined in a 3D or 2D space. Two of the Tamura texture measures are *coarseness* and *directionality* [28]. Recent studies [29, 30] also suggest that they are among the few most effective perceptual dimensions in discriminating texture patterns.

   In our edge-based approach, the directionality is simply measured by the gradient direction ϕ of the edge pixels. It is especially useful in handling rotations. When an object is rotated on a 2-D plane (e.g., a book is placed on the desk with a different orientation), all the edge orientations are simply incremented (or decremented) by a θ. The coarseness can be characterized by *edge separation* which is measured by the distance of the nearest edge pixel along the direction of ϕ. Apparently, the edge separation is sensitive to the scale/resolution of the images.

   The current C-BIRD implementation uses a 2D texture space which is composed of S (edge separation) and ϕ (directionality). The texture statistics are extracted for each locale; in other words, they are *locale-based*. They are derived from the edge image of the luminance image Y, where $Y = 0.299R + 0.587G + 0.114B$.

3. Shape: The Generalized Hough Transform (GHT) [31] is adopted to represent the shape of the object. Briefly, each edge point in the object model is represented by a vector $\mathbf{r}_i(\psi_i, r_i)$ connecting the edge point to a chosen reference point for the object. All $\mathbf{r}_i$'s are stored in an R-table which serves as an object model. The R-table is indexed by the edge orientation ϕ_i of the edge point. At the matching time, each edge point in the database image uses the R-table to cast its vote to an accumulate array. As a result, a peak will be formed at the location of the corresponding reference point in the accumulate array if the object indeed appears in the database image.

   The major advantage of the GHT (and its variants) over other shape representations [32] is its insensitivity to noise and occlusion [33, 34]. It can also be applied hierarchically to describe the object (or a portion of the object) at multiple resolutions. It is known that the discriminative power of the GHT diminishes when the aim is to recognize the object at all possible scales and orientations, because then the GHT matching will have to be attempted at numerous iterations and the decision often becomes non-attainable. We will hence propose the following three-step matching algorithm in which the GHT will only be applied after the first two steps when a certain hypothesis of a possible object size, orientation, and location is made.

4.2 The three-step matching algorithm

A three-step matching algorithm for searching by object models in image and video databases is developed, i.e., (1) color hypothesis, (2) texture support, (3) shape verification. It is generally accepted that color is fairly invariant to scaling and rotation, hence the feature color is used in the first step of the matching. After color localization, a hypothesis of the existence of an object at a certain location, size and orientation can be made. If there is a sufficient similarity in their texture between the object model and the image at the vicinity of the hypothesized enclosure, then a shape verification procedure based on the GHT will be invoked.

For both color and shape, there is an issue of *similarity*. It is dealt with effectively using the MFC vectors and the geometric and texture parameters of the locales. First, if the model object appears in the image with exactly the same size and orientation, then the mass M, eccentricity E of each locale, the length ρ_i and orientation α_i of each MFC vector, and the angles β_j between the pairs of the MFC vectors are all identical, whether they are extracted from the model or from the object in the image. Second, if the object in the image has a different size and/or orientation, then M and ρ_i should be scaled according to the size ratio, α_i should be incremented by a rotational angle θ, whereas β_j would remain the same. Certain tolerance for error is implemented to support the similarity.

In summary, the matching algorithm is as below:

Matching Algorithm:

```
begin
    /* Image tile generation */
    Within each 16 × 16 tile of an image
        Gather M, C, E for each MFC associated with the object model;

    /* Color localization */
    Use overlapped pyramid linking to group tiles into locale ℒ's for each MFC;

    /* Color hypothesis */
    If (#-of-similar-color-locales ≥ 2) and their MFC-vectors
    are 'similar' to the MFC-vectors in the model
        Make hypothesis of size, orientation, and bounding-box of a matching object;

    /* Texture support */
    For all locales of the hypothesized matching object
        if texture measures are consistent with the hypothesized size and orientation
            Proceed to check the shape using the GHT;

    /* Shape verification*/
    Within (and at the vicinity of) the hypothesized bounding-box
        All edge pixels use R-table of the (rotated/scaled) object model to vote;
        If #-of-votes near the reference point exceeds a chosen threshold
            Confirm the detection of the object;
end
```

4.3 Specifics for search by object model

4.3.1 Locale-based texture measure

Texture statistics is gathered under each envelope/locale. We use edge detection and separation algorithms on the full-resolution image. No downsampling is applied at this step because texture is very resolution-dependent. To generate an edge-map we use the Sobel edge operators and a non-maxima edge suppression. A global threshold for edge detection applying to the entire image often yields poor results. In particular, the amount of edges for the object model could be severely affected by the possibly varying background, which will directly affect the texture measures. In C-BIRD, edge detection is conducted within individual locales (and their immediately surrounding areas to detect the possible boundary edge pixels of the locales). We threshold the edge-map using the median of the intensity values of the edge pixels inside each envelope. The Application of the local threshold for each locale improves the consistency of the edge detection and hence the quality of the texture measure.

To generate the S (edge separation) information, for every edge pixel in an envelope we measure the pixel distance from it along its gradient line to the closest edge pixel inside the same envelope that has a similar gradient angle within a threshold of $15°$. The distances from both sides of the pixel (along ϕ and $\phi + 180°$) are taken into account. If there is no other edge pixel along the gradient line, then the separation distance is 'infinity'. Also, if the separation is larger than a specified maximum (192 pixels for 640×480 images), then S is considered to be 'infinity'.

A histogram of S (edge separation) vs. ϕ (edge gradient angle / directionality) is created for the texture measure of each locale. The texture histograms is normalized by simply using percentage values. Initially, the size of the histograms is 193×180, where $S = 193$ refers to infinity. For efficiency, the histograms are later greatly subsampled. To reduce the impact of noises and the inevitable deviations between the model and the object in the database, the texture histograms are also smoothed by applying a Gaussian operator. The resulting histogram is quantized at 9×8, where S axis is divided into 8 cells plus the ninth cell for the infinity, and the ϕ axis is divided into 8 cells.

4.3.2 Estimation of scale and rotation & execution of the GHT

The database images are screened by considering only the images that have all the locale colors of the model image. Let $M(\mathcal{L}^m_{MFC_1})$, $M(\mathcal{L}^m_{MFC_i})$, $M(\mathcal{L}^{db}_{MFC_1})$, and $M(\mathcal{L}^{db}_{MFC_i})$ denote the mass of the first and ith MFCs from the model image and the database image respectively, MFV^m_{i-1} and MFV^{db}_{i-1} the $(i-1)$th vectors that connect the centroids of these MFC locales. For each pair of the MFC vectors from the model image and the database image, the following are checked to determine whether a hypothesis of the existence of an object with a certain scale and orientation is warranted:

If $\sqrt{M(\mathcal{L}^{db}_{MFC_1})/M(\mathcal{L}^{m}_{MFC_1})} = k$, then

$\sqrt{M(\mathcal{L}^{db}_{MFC_i})/M(\mathcal{L}^{m}_{MFC_i})} \approx k$ and $\left|MFV^{db}_{i-1}\right| / \left|MFV^{m}_{i-1}\right| \approx k$;

and if $\alpha(MFV^{db}_1) - \alpha(MFV^{m}_1) = \theta$ then

$\alpha(MFV^{db}_{i-1}) - \alpha(MFV^{m}_{i-1}) \approx \theta$.

The "≈" symbol allows error tolerance of the above measures. A simple weighted average error is used to determine whether it passes the threshold for the "Color Hypothesis" step. If successful, then the weighted average scale factor $\bar{k}$ and rotation $\bar{\theta}$ are employed as the hypothesized scale and rotation factors.

The texture histograms for each pair of the matching locales from the model image and the database image are compared after the adjustment according to $\bar{k}$ and $\bar{\theta}$. Namely, in the database texture histogram the angle value is incremented by $\bar{\theta}$, and the separation value is multiplied by $\bar{k}$.

As in the color histogram matching (Eq. (2)), the texture histograms $\boldsymbol{H}^{m}_{i}(\bar{k}, \bar{\theta})$ and $\boldsymbol{H}^{db}_{i}(\bar{k}, \bar{\theta})$ are matched by *histogram intersection*, i.e., by taking the sum of the minimum of the texture histograms.

$$\nu \equiv \sum_{\bar{k}, \bar{\theta}} min\{\boldsymbol{H}^{m}_{i}(\bar{k}, \bar{\theta}), \boldsymbol{H}^{db}_{i}(\bar{k}, \bar{\theta})\} \tag{6}$$

If $\nu >$ threshold τ_0, then the "Color Hypothesis" has the "Texture Support".

The implementation of the Generalized Hough Transform (GHT) is fairly straight-forward [31], except

1. the GHT is only performed on a portion of the database image at the location containing all of the matched locales to save time;

2. the voting for the GHT is only for the single scale and rotation $\bar{k}$ and $\bar{\theta}$.

After the GHT voting, the accumulate array is smoothed (i.e., every 5×5 neighborhood is averaged) to aid the peak allocation. The maximum value in the accumulate array is then located. If it exceeds the threshold (50% of total edges in the R-table for the object, adjusted by $\bar{k}$), then its location indicates the location of the matched object in the database image.

5 Experimental Results

This section demonstrates some of our preliminary results.

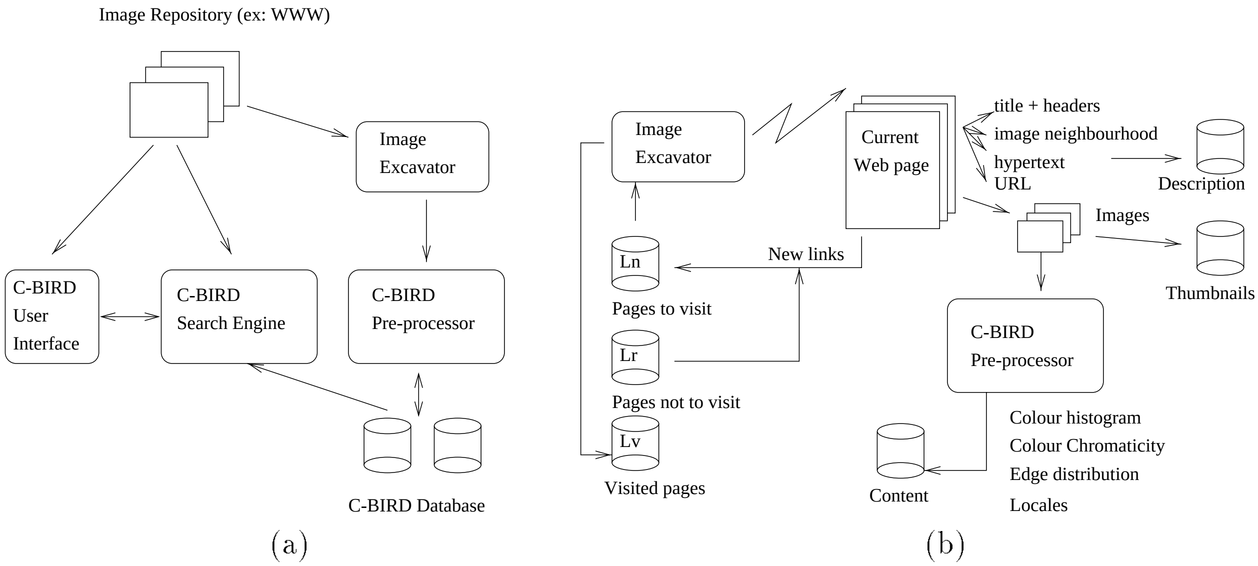

Figure 2: (a) C-BIRD general architecture. (b) Excavator: The Web crawling process for image extraction.

5.1 General descriptions on system design

The C-BIRD system has been implemented on both Unix and PC platforms. On both platforms, we used the same search engine and pre-processor written in C^{++}. The user interface is implemented in Perl and HTML as a Web application using any Web browser, as well as a java applet. Figure 2 shows the general architecture for C-BIRD implementation. The system is accessible from http://jupiter.cs.sfu.ca/cbird/cbird.cgi, and http://jupiter.cs.sfu.ca/cbird/java/ (IE 4.0 or Netscape 4.0).

C-BIRD system rests on 4 major components:

- Extraction of images from the WWW (Image Excavator);
- Processing of images to extract image features and storing precomputed data in a database (Pre-Processor);
- Querying (User Interface);
- Matching query with image features in the database (Search Engine).

The Image Excavator extracts images from an image repository. This repository can be the WWW space, in such case, the process crawls the Web searching for images, or a set of still images on disk or CD-ROM. Frames can also be extracted from video streams using cut-detection algorithms [35, 18, 6] and processed as still images. Once images are extracted from the repository, they are given as input to the image analyzer (C-BIRD pre-processor) that extracts visual content features like color and edge characteristics. These visual features, along with the context feature like image URL, parent URL, keywords, etc., extracted with the Image Excavator, are stored in a database. The collection of images and the extraction of image features are processes that are done off-line before queries are submitted. When a query is submitted, accessing the original data in the image repository is not necessary. Only the precomputed data stored in the database is used for image feature matching. This makes C-BIRD more scalable and allows fast query responses for a large number of users and a huge set of images.

We have implemented several types of searches and any combinations of them in C-BIRD:

1. Search by conjunctions and disjunctions of keywords;

2. Search by color histogram: similarity with color histogram in a sample image. Color can also be specified in percentage within the image or layout in a 1×1. 2×2, 4×4 or 8×8 grid;

3. Search by texture: texture here is characterized by edge density and orientation, its layout can also be specified;

4. Search by illumination invariance: similarity with color chromaticity using color-channel-normalized images;

5. Search by object model: specification of an object to look for in images.

The left of Figure 3(a) shows the user interface using Netscape to browse the image repository or the image set resulting from a query. While browsing, users can submit a query by image similarity. The right of Figure 3(a) shows a user interface to specify color layout for a given query. Figure 3(b) shows an example of an output (images and their associated keywords) from the Image Excavator after parsing a web page.

The Image Excavator is a web crawler that we built to follow links from web page to web page in search of images. The text present in each web page is parsed and some representative keywords are retained and associated to the images found in the web page. The keyword

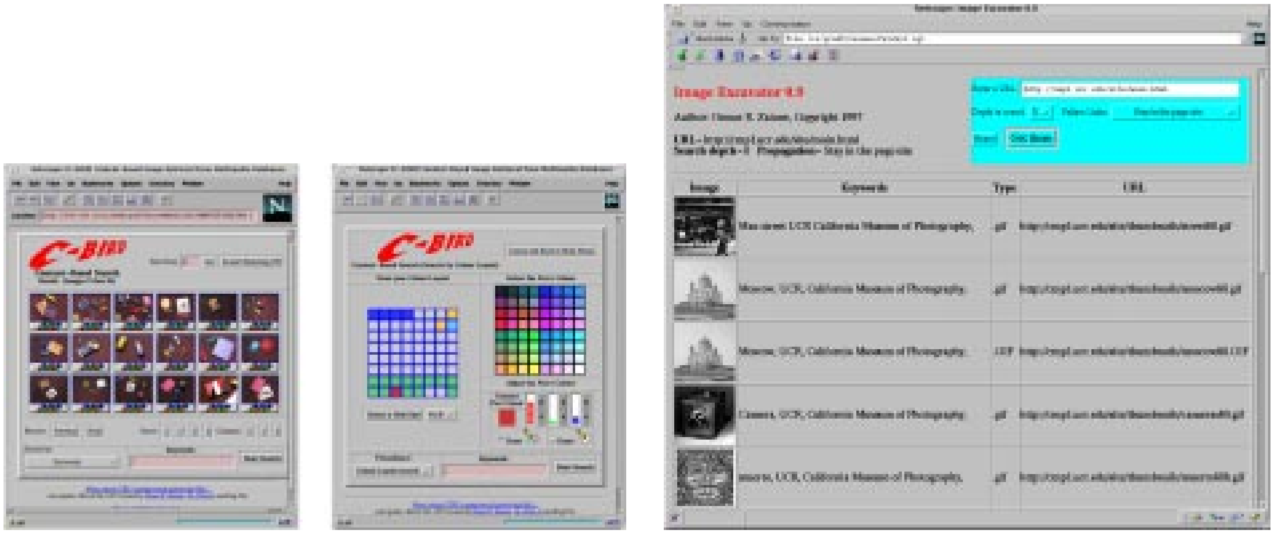

(a) (b)

Figure 3: (a) C-BIRD Web user interface. (b) Output from the Image Excavator

extraction process uses a semantic network of English words and builds concept hierarchies with the selected words. The process of keyword extraction is explained in [36, 37].

The database used by C-BIRD contains mainly meta-data extracted by the pre-processor and the Image Excavator. As explained above, only features collected in this database at pre-processing time, are used by the search engine for image or image feature matching. During run time, minimal processing is done. For each image collected, the database contains some description information, a feature descriptor, and a layout descriptor, as well as a set of multi-resolution sub-images (i.e. search windows) feature descriptors. Neither the original image nor the sub-images are directly stored in the database but only their feature descriptors.

We use our illuminance invariant method to detect cuts in videos, and segment a video into clips (frame sequences). The starting time and duration of the image sequence are stored with the meta-data. While the thumbnail is generated from the middle frame of the clip, color and texture features are extracted from all frames.

The current test database has over 1,300 images. The meta-data is stored in a SQL server running on a Pentium-II 333 MHz PC with 128 MB of RAM. Search times are in the order of 0.1 to 2 seconds depending upon the type of search, except for the search by object, which may take up to 10 seconds.

Figure 4 demonstrates the use of conjunction of different searches, content-based and description-based. Figure 4(a) is the the top-20 matches of a query based on the color layout

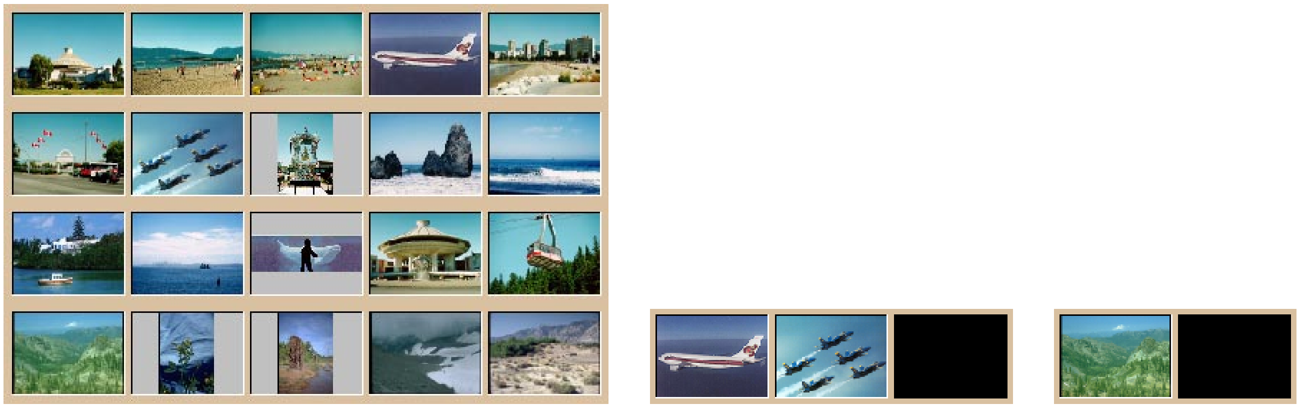

(a) (b) (c)

Figure 4: Conjuction of searches.

(a) (b)

Figure 5: Comparison of two results: (a) Result of Search by Color Histogram, (b) Result of Search by Illumination Invariance.

where the top cells were blue (i.e. for blue sky). Figure 4(b) is the result for a combination of content-based and description-based query, with “blue sky” specified as for Figure 4(a) and an additional keyword “airplane”. Figure 4(c) is the result of the query “blue sky and green grassland” specified with a color layout grid with the top cells blue, the bottom cells green and a medium edge density.

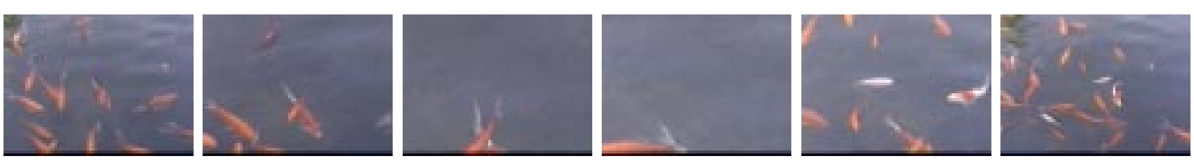

Figure 6: Selected frames of a video clip.

5.2 Search by illumination invariance

The experimental results for Search by Illumination Invariance are very promising. Figure 5 provides a comparison between the ordinary Search by Color Histogram and our Search by Illumination Invariance. The image sample selected for both searches is the first T-shirt image which is taken under a dim bluish light. The entire database is searched and the first 15 matches (sometimes mismatches) are shown in descending order of their matching scores. As expected, the by-color-histogram method (Figure 5(a)) is only capable of turning out many dark images, of which the third image happens to be a correct match (the same T-shirt being folded slightly differently and rotated). However, its matching score ranks behind a book. The result of by-illumination-invariance shown in Figure 5(b) is far better. All three occurrences of the sample T-shirt, the third one under a redish light, are found. Notably, it also finds many T-shirts under various illuminations. Since the sample T-shirt has basically two colors (dark stripes on white cloth), the matches are mostly correct in terms of their chromaticities, albeit unexpected.

Figure 6 depicts some selected frames from a clip of 'goldfish' scene in a 3-minute video that contains 22 cuts/clips. Because the camera was chasing the fish, the reflectance changes significantly. By selecting the threshold very carefully, the color histogram method still missed one cut and mistakenly added three more cuts (one of them at the third frame in the goldfish clip shown). As shown in [18] the color histogram is simply not able to satisfy both the precision and recall in video segmentation. Our illumination invariant method, however, detects all cuts correctly using a fixed threshold which works for other test videos as well.

5.3 Search by object model

5.3.1 Locale construction

The Locale construction algorithm is implemented in the C-BIRD system. Its threshold parameters are chosen to be optimized for the average object size, although they also work well for objects up to 5 times the magnitude scale. The execution speed of the method is fairly fast (less than a second for each 640×480 image). In all images tested, most of the Locales correctly enveloped features, and separated similar features of different objects from each other or background noise. We present here the results from each step in the Locale construction method as applied to a sample image.

Figure 7: The dominant colors identification algorithm is applied to the sample image shown in A. On the top, portion of the result image is amplified for display. A. The original image. B. The image with only dominant pixels, all other pixels are grey. C. The image with both the dominant pixels and the transitional pixels that assume a dominant color.

We first identify the pixels with dominant colors and the colors that the transitional pixels would merge into. The results are presented in Figure 7. It is shown that transitional pixels are changed to the closest dominant color in their neighborhood.

We generate the image tiles array using the dominant colors we identified, and then generate all the Locales for the image. The Locales are shown in Figure 8. Most features are correctly enveloped.

5.3.2 Result of the three-step matching algorithm

Figure 9 and Figure 10 illustrate an example of the three-step matching in Search by Object Model. The 'pink book' model is shown in Figure 9(a). One of the database books is in Figure 9(b), the actual rotation of the book is 55°, and the actual scale is 1.37. The hypothesized rotation $\bar{\theta}$ is 60° and scale $\bar{k}$ is 1.44; the rotation disparity between the two MFC vectors is 20°, and the scale disparity among the MFCs and MFC vectors is 0.1. The texture measure ν values for all three locales exceed the threshold of 50% (with 100% representing a perfect match). Hence, the third step — Shape Verification is carried out.

The GHT matching result is illustrated in Figure 10. With the hypothesized $\bar{\theta}$ and $\bar{k}$, the GHT matching takes very little time. The brightest spot represents the highest vote

Figure 8: The Locales generated for the sample image in Figure 7. Every image shows a different Locale which is composed of the color tiles.

(a) (b)

Figure 9: Illustration of the MFCs and MFC Vectors. (a) The 'pink book' model image: the pink locale has a mass of 21,352 pixels and centroid at (78, 122), the white locale has a mass of 6,564 pixels and centroid at (82, 86), and the purple locale has a mass of 1,236 and centroid at (70, 108). (b) One of the database images: the pink locale has a mass of 40,522 pixels and centroid at (440, 194), the white locale has a mass of 12,644 pixels and centroid at (394, 172), and the purple locale has a mass of 1,992 and centroid at (416, 206).

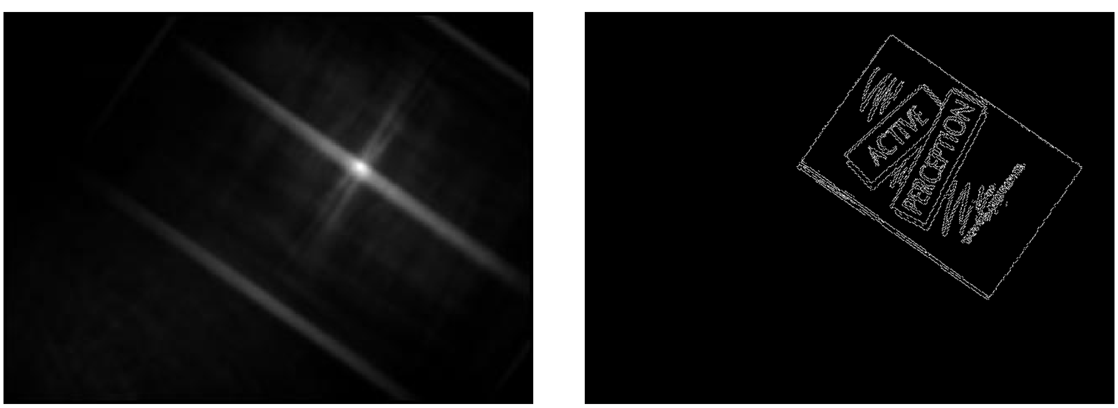

(a) (b)

Figure 10: Result of the Generalized Hough Transform. (a) A gray-level encoded display for the GHT accumulate array. The brightest spot represents the highest vote count (the peak) and it corresponds to the reference point of the pink book. (b) A regenerated edge map of the detected book.

count (close to 70% of the number of edges in the model images) and it corresponds to the reference point of the pink book. The (relatively) bright stripes also indicate high vote counts, they are caused by the many edge pixels along the straight boundaries of the book, and (correctly) they are not as large as the vote counts at the peak. Figure 10(b) depicts a regenerated edge map at the location of the detected book. The result is quite satisfactory in spite of the slight errors of the book's scale and orientation.

Figure 11 shows the result for the query "find the above pink book from all images (over 1,300) in the database". As shown, 4 of the 5 occurrences of this book with various sizes, positions and orientations are correctly retrieved. The fifth pink book is hypothesized at the first two steps and then rejected at the GHT step. It is because the white area next to the top of the pink book was merged with the white locale of the book, which caused enough hardship for our current implementation.

We have so far worked with rectangular shaped books as our models. Our three-step algorithm however does not rely on any simple shape such as a rectangle, especially when the GHT is used for shape matching. In our JAVA interface, users are also able to crop out any object/pattern in any image and use it as a model to search.

Several content-based image and video retrieval systems use region-based search methods. For example, QBIC [2] uses rectangular shaped colored regions; Video-Q [8] keeps the description and spatial relationship of regions, so that user can sketch the trajectory of moving color regions for the retrieval of certain moving objects. These systems rely heavily on a good segmentation preprocess and they do not have a systematic means of retrieving objects. To the best of our knowledge, C-BIRD is the first system that successfully performs object model search from image and video databases.

6 Conclusion and Discussion

Content-based image and video retrieval is an important issue in the research and development of digital libraries which usually employ large multimedia databases. This paper presented our prototype system C-BIRD for content-based image retrieval from large image and video databases. Issues in both database design and image content based retrieval are addressed. Two unique features for C-BIRD, i.e., Search by Illumination Invariance and Search by Object Model, are discussed in detail.

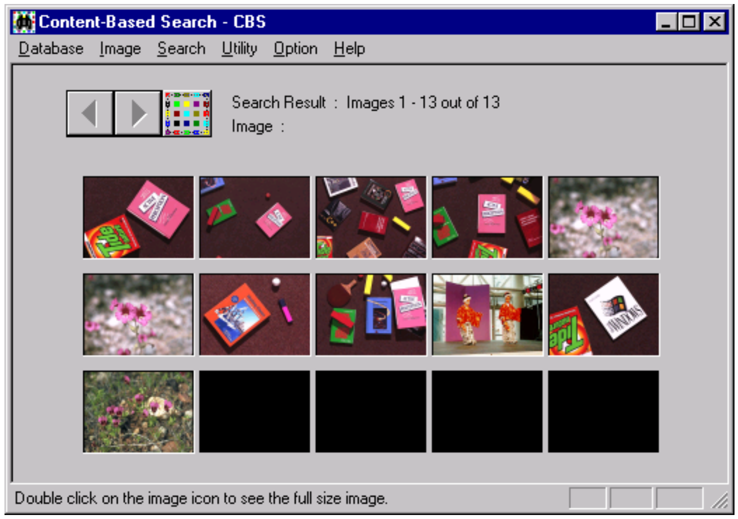

(a) Retrieved images after the Color Hypothesis

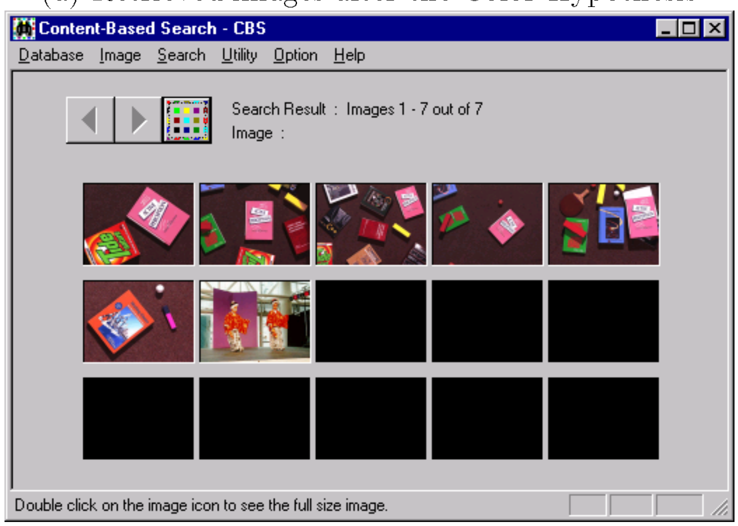

(b) Images that also have Texture Support

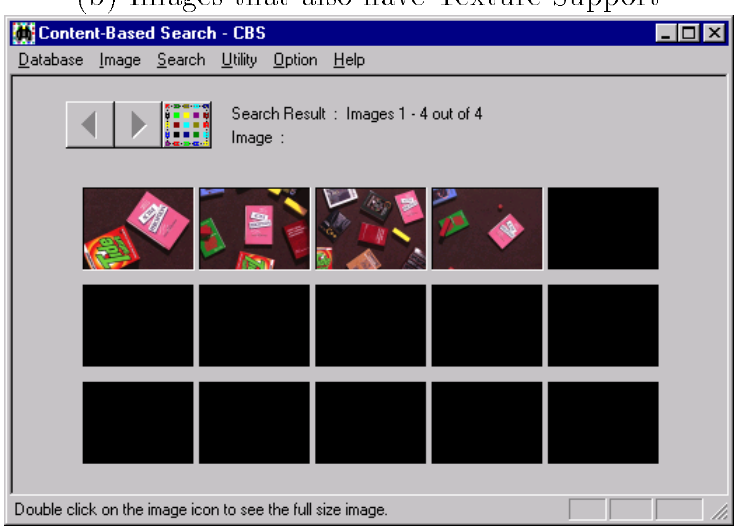

(c) Images that finally pass the GHT step

Figure 11: Result of the three-step matching.

First, the simple idea of normalizing color images separately in each band is adopted as a reasonable approach to color constancy preprocessing in the context of indexing in image and video databases. We transform to a 2D representation by using histograms of chromaticity. Viewing these 2D feature space histograms as images, we apply a wavelet–based image reduction transformation for low–pass filtering, followed by DCT and truncation. The resulting indexing scheme uses only 36 integers as feature vectors to index into the image database and hence is very efficient. Experiments show good results because of the illuminant-invariance.

Second, feature localization and a three-step matching algorithm are presented to support Search by Object Model. Unlike most existing systems which use only features (color, texture, sketch, etc.) to retrieve similar images, the modeling and matching methods described are capable of retrieving a range of different sizes, 2-D rotations, and multiple occurrences of specified objects in the images. It is shown that instead of image segmentation, feature localization should be used as a preprocessing step before matching.

We are currently expanding our database to include more images and videos, especially to automate the Web crawling process. The precision and recall of the C-BIRD system from our current database are satisfactory. A more comprehensive analysis on them will be undertaken with the expanded database. At present, only models of 2D objects are supported. Further study on 3D modeling and matching will be a major challenge as it has been for the last few decades to the computer vision research community.

Acknowledgments: This work was supported in part by the Canadian National Science and Engineering Research Council under the grant OGP-36727, and the grant for Telelearning Research Project in the Canadian Network of Centres of Excellence.

References

[1] A. Pentland, R.W. Picard, and S. Sclaroff. Photobook: Tools for content-based manipulation of image databases. In *SPIE Storage and Retrieval for Image and Video Databases II*, volume 2, 185, pages 34–47, San Jose, CA, 1994.

[2] M. Flickner, H. Sawhney, W. Niblack, and et al. Query by image and video content: The QBIC system. *IEEE Computer*, pages 23–32, September 1 1995.

[3] H.J. Zhang, et al. Automatic parsing and indexing of new video. *Multimedia Systems*, 2(6):256–266, 1995.

[4] J.R. Bach, C. Fuller, A. Gupta, and et al. The Virage image search engine: An open framework for image management. In *SPIE Storage and Retrieval for Image and Video Databases IV*, February 1996.

[5] C. Frankel, M. J. Swain, and V. Athitsos. Webseer: An image search engine for the world wide web. Technical Report 96-14, University of Chicago, Computer Science Department, August 1996.

[6] P. Aigrain, H. Zhang, and D. Petkovic. Content-based representation and retrieval of visual media: A state-of-the-art review. *Int. J. Multimedia Tools and Applications*, 3:179–202, November 1996.

[7] J.R. Smith and S.F. Chang. Visually searching the web for content. *IEEE Multimedia*, 4(3):12–20, 1997.

[8] S.F. Chang, et al. VideoQ: an automated content based video search system using visual cues. In *Proc. ACM Multimedia 97*, pages 313–324, 1997.

[9] S. Mukherjea, K. Hirata, and Y. Hara. Toward a multimedia world wideweb information retrieval engine. In *Sixth Int. Worl-Wide Web Conf.*, Santa Clara, CA, 1997.

[10] E. Selberg and O. Etzioni. Multi-service search and comparison using the metacrawler. In *4th International World Wide Web Conference*, 1996.

[11] G. Furnas, T.K. Landauer, L.M. Gomez, and S. Dumais. The vocabulary problem in human-system communications. *Communications of the ACM*, 30:964–971, 1987.

[12] C. Frankel, M. Swain, and V. Athitsos. Webseer: An image search engine for the World Wide Web. Technical Report TR-96-14, CS Department, Univ. of Chicago, 1996.

[13] K. Hirata, Y. Hara, N. Shibata, and F. Hirabayashi. Media-based navigation for hypermedia systems. In *Proceedings of ACM Hupertext'93 Conf.*, pages 159–173, Seattle, WA, 1993.

[14] M.J. Swain and D.H. Ballard. Color indexing. *Int. J. Computer Vision*, 7(1):11–32, 1991.

[15] B.V. Funt and G.D. Finlayson. Color constant color indexing. *IEEE Trans. Patt. Anal. and Mach. Intell.*, 17:522–529, 1995.

[16] M.S. Drew, J. Wei, and Z.N. Li. Illumination–invariant color object recognition via compressed chromaticity histograms of color–channel–normalized images. In *Proc. Int. Conf. on Computer Vision (ICCV '98)*, pages 533–540, 1998.

[17] A.M. Tekalp. *Digital video processing.* Prentice Hall PTR, 1995.

[18] J. Wei, M.S. Drew, and Z.N. Li. Illumination invariant video segmentation by hierarchical robust thresholding. In *Proc. IS&T/SPIE Symp. on Electronic Imaging '98, Storage & Retrieval for Image and Video Databases VI, SPIE Vol. 3312*, pages 188–201, 1998.

[19] R.L. Gregory. *The Intelligent Eye.* Weidenfeld & Nicholson, 1970.

[20] D. Marr. *Vision.* W. H. Freeman, 1982.

[21] R. Chellappa and A. Rosenfeld. Computer vision: attitude, barriers, counseling. In *Proc. Vision Interface '92*, pages 1–7, 1992.

[22] W.Y. Ma and B.S. Manjunath. Edge flow: a framework of boundary detection and image segmentation. In *Proc. IEEE Conf. on Computer Vision and Pattern Recognition*, pages 744–749, 1997.

[23] G. Wyszecki and W.S. Stiles. *Color Science: Concepts and Methods, Quantitative Data and Formulas, 2nd ed.* Wiley, New York, 1982.

[24] M. Antonini, et al. Image coding using wavelet transform. *IEEE Trans. on Image Processing*, 1(2):205–221, 1992.

[25] D.H. Ballard and C.M. Brown. *Computer Vision.* Prentice Hall, 1982.

[26] T.H. Hong and A. Rosenfeld. Compact region extraction using weighted pixel linking in a pyramid. *IEEE Trans. on Pattern Analysis and Machine Intelligence*, PAMI-6(2):222–229, 1984.

[27] Z.N. Li and B. Yan. Recognition kernel for content-based search. In *Proc. IEEE Conf. on Systems, Man, and Cybernetics*, pages 472–477, 1996.

[28] H. Tamura, S. Mori, and T. Yamawaki. Texture features corresponding to visual perception. *IEEE Trans. on Systems, Man, and Cybernetics*, 8(6):460–473, 1978.

[29] A.R. Rao and G.L. Lohse. Towards a texture naming system: identifying relevant dimensions of texture. In *Proc. IEEE Conf. on Visualization*, pages 220–227, San Jose, 1993.

[30] F. Liu and R.W. Picard. Periodicity, directionality, and randomness: Wold features for image modeling and retrieval. *IEEE Trans. on Pattern Analysis and Machine Intelligence*, 18(7):722–733, 1996.

[31] D. Ballard. Generalizing the Hough transform to detect arbitrary shapes. *Pattern Recognition*, 13(2):111–122, 1981.

[32] J. Ostermann, E.S. Jang, J. Shin, and T. Chen. Coding of arbitrarily shaped video objects in MPEG-4. In *Proc. Int. Conf. on Image Processing (ICIP '97)*, pages 496–499, 1997.

[33] Z.N. Li, B.G. Yao, and F. Tong. Linear generalized Hough transform and its parallelization. *Image and Vision Computing*, 11(1):11–24, 1993.

[34] P. Gvozdjak and Z.N. Li. From nomad to explorer: Active object recognition on mobile robots. *Pattern Recognition*, 31(6):773–790, 1998.

[35] N. Hirzalla and A. Karmouch. Detecting cuts by understanding camera operations for video indexing. *Journal of Visual Languages and Computing*, 6:385–404, 1995.

[36] O. R. Zaïane, A. Fall, S. Rochefort, V. Dahl, and P. Tarau. On-line resource discovery using natural language. In *Proceedings, RIAO'97*, Montreal, Canada, June 1997.

[37] O. R. Zaïane, J. Han, Z-N. Li, J. Hou, and G. Liu. Mining multimedia data. In *CASCON'98: Meeting of Minds*, Toronto, Canada, November 1998. submitted for review.